JACS
JOURNAL OF THE AMERICAN CHEMICAL SOCIETY
Communication
pubs.acs.org/JACS

An Exceptionally Fast Homogeneous Carbon-Free Cobalt-Based Water Oxidation Catalyst

Hongjin Lv,[†,⊥] Jie Song,[†,⊥] Yurii V. Geletii,[†] James W. Vickers,[†] Jordan M. Sumliner,[†] Djamaladdin G. Musaev,[‡] Paul Kögerler,[§] Petro F. Zhuk,[∥] John Bacsa,[†] Guibo Zhu,[†] and Craig L. Hill*[,†]

[†]Department of Chemistry and [‡]Emerson Center for Scientific Computation, Emory University, 1515 Dickey Dr., Atlanta, Georgia 30322, United States,

[§]Institut für Anorganische Chemie, RWTH Aachen University, D-52074, Aachen, Germany

[∥]National Aviation University, Kiev, Ukraine 03680

Supporting Information

ABSTRACT: An all-inorganic, oxidatively and thermally stable, homogeneous water oxidation catalyst based on redox-active (vanadate(V)-centered) polyoxometalate ligands, $Na_{10}[Co_4(H_2O)_2(VW_9O_{34})_2]\cdot 35H_2O$ (Na_{10}**1-V2**, sodium salt of the polyanion **1-V2**), was synthesized, thoroughly characterized and shown to catalyze water oxidation in dark and visible-light-driven conditions. This synthetic catalyst is exceptionally fast under mild conditions (TOF > 1×10^3 s^{-1}). Under light-driven conditions using $[Ru(bpy)_3]^{2+}$ as a photosensitizer and persulfate as a sacrificial electron acceptor, **1-V2** exhibits higher selectivity for water oxidation versus bpy ligand oxidation, the final O_2 yield by **1-V2** is twice as high as that of using $[Co_4(H_2O)_2(PW_9O_{34})_2]^{10-}$ (**1-P2**), and the quantum efficiency of O_2 formation at 6.0 μM **1-V2** reaches ~68%. Multiple experimental results (e.g., UV−vis absorption, FT-IR, ^{51}V NMR, dynamic light scattering, tetra-*n*-heptylammonium nitrate-toluene extraction, effect of pH, buffer, and buffer concentration, etc.) confirm that the polyanion unit (**1-V2**) itself is the dominant active catalyst and not Co^{2+}(aq) or cobalt oxide.

The development of fast, selective, and stable water oxidation catalysts (WOCs) continues to be centrally important to the conversion of light energy into chemical energy.[1−5] As a consequence, there has been substantial work on both homogeneous[6−17] and heterogeneous[18−29] WOCs. Insightful recent studies of Ru-[28] and Co-based[29] WOCs with organic ligands show very high base-dependent catalytic water oxidation rates (~10^3). In recent years, many carbon-free, robust, molecular WOCs comprising polydentate polyoxometalate (POM) ligands stabilizing a mononuclear or polynuclear transition metal cores have been reported.[7,30−47] This family of catalysts eliminates the problem of ligand oxidative instability, while being very stable thermally and readily immobilized on a variety of electroactive surfaces;[33,48,49] however, they are still slow for use in efficient artificial photosynthetic systems. Here, we report the synthesis, characterization, and water oxidation activity of the carbon-free homogeneous WOC, $[Co_4(H_2O)_2(VW_9O_{34})_2]^{10-}$ (**1-V2**). The complex **1-V2** is prepared from a mixture of earth-abundant materials: cobalt ions, vanadate ($NaVO_3$), and tungstate (Na_2WO_4) in aqueous solution (see Supporting Information (SI) for details). Following an earlier report,[50] we have critically revisited and significantly improved the X-ray crystallographic and magnetic characterization of **1-V2** and confirmed that it is isostructural to the previously reported, $[Co_4(H_2O)_2(PW_9O_{34})_2]^{10-}$ (**1-P2**; Figure S1).[6,7] In both complexes, **1-V2** and **1-P2**, two trilacunary B-type $[XW_9O_{34}]^{9-}$ (X = V or P) ligands sandwich a tetra-cobalt cluster $[Co_4O_{14}]$. Two of the Co(II) centers on the outside positions in this central unit are solvent accessible and consequently bear one terminal aqua (water) ligand each. To our knowledge, the *R* value of 2.43% of our X-ray structure of K_{10}**1-V2** is one of the lowest ever reported for a polyoxometalate so that the hydrogens on the cobalt terminal aqua ligands have been located (Figure 1, Table S1). The VO_4 unit in each $[VW_9O_{34}]^{9-}$ ligand has an approximately tetrahedral structure. Bond valence sum (BVS) calculations show that all the cobalt and the vanadium centers are in the 2+ and 5+ oxidation states, respectively (Table S2). Extensive spectroscopic data on **1-V2** confirm the structure from the X-ray diffraction study (see SI for details). The ^{51}V NMR spectrum of **1-V2** shows only one peak at −506.8 ppm ($\Delta\nu_{1/2}$ = 30.5 Hz) for the central pseudotetrahedral V in the two symmetry-equivalent $[VW_9O_{34}]^{9-}$ ligands (Figure S7). The

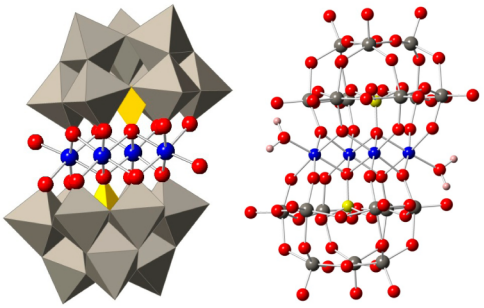

Figure 1. X-ray crystal structure of **1-V2** in combined ball-and-stick and polyhedral representations. Red: oxygen; blue: cobalt; yellow: VO_4 or V; gray: WO_6 or W.

Received: May 7, 2014
Published: June 17, 2014

   dx.doi.org/10.1021/ja5045488 | *J. Am. Chem. Soc.* 2014, 136, 9268−9271

ESI-MS spectra for the TBA salt of **1-V2** also confirm this structure: the assignments of the main peak envelopes indicate the presence of the **1-V2** polyanions in solution (Figure S9 and Table S3).

Although both **1-V2** and **1-P2** have the same charge (10−) and very similar geometrical structures (metal−oxygen connectivity), they exhibit different electronic structures. First, the UV−vis spectrum of **1-V2** reveals transitions involving orbitals with both cobalt and heteroatom (vanadium) character in aqueous solution or in 80 mM borate buffer, whereas, the spectrum of **1-P2** does not. The ligand-to-metal charge transfer (LMCT) and d−d transitions for **1-V2** are at 400 nm (ε_{400} = 1323 M^{-1} cm^{-1}) and 580 nm (ε_{580} = 158 M^{-1} cm^{-1}) respectively; whereas those for **1-P2** are at 580 nm (ε_{580} = 158 M^{-1} cm^{-1}) (Figure S4). Second, DFT calculations reveal that (a) the ground electronic state of **1-V2** is ^{13}A with four Co^{2+} centers, (b) its highest single occupied molecular orbitals (Figure S11) are primarily the d-orbitals of Co centers, with some mixing of oxygen orbitals of the $\{VW_9O_{34}\}$ units) followed by doubly occupied oxygen orbitals of $\{VW_9O_{34}\}$ units and doubly occupied Co atomic orbitals, and (c) the lowest unoccupied orbital of **1-V2** contains mainly the VO_4 orbitals with some mixture from the Co_4O_x belt. This implicates the direct role of the d^0, V(V) centers in any redox chemistry of **1-V2**. No analogous orbital is found in **1-P2**. The calculated important bond distances are in good agreement with their X-ray crystallographic values (Figure S10 and Table S1). Third, a full temperature-dependent magnetism study of **1-V2** and **1-P2** reveals significant differences in the two complexes (see Figures S12 and S13), which reflect differences in the frontier orbitals involving the μ-O bridges linking the Co^{2+} spin centers that in turn translate into different coupling energies: whereas all nearest-neighbor interactions in **1-V2** are ferromagnetic, both ferromagnetic and weak antiferromagnetic couplings are found for **1-P2**. Overall, electronic structure data obtained from the full temperature-dependent magnetism study are consistent with aforementioned computational findings.

The catalytic efficiency of **1-V2** and **1-P2** for water oxidation has been evaluated using $[Ru(bpy)_3]^{3+}$ as a stoichiometric oxidant in eq 1 by following the kinetics of $[Ru(bpy)_3]^{3+}$ (ε_{670} = 420 M^{-1} cm^{-1})[51] consumption in 80 mM borate buffer at pH 9.0 using the stopped-flow technique (Figure 2, Figure S14).

$$4[Ru(bpy)_3]^{3+} + 2H_2O \rightarrow 4[Ru(bpy)_3]^{2+} + O_2 + 4H^+ \quad (1)$$

The kinetic curves for the catalytic process are not exponential; the reaction is inhibited by product $[Ru(bpy)_3]^{2+}$. In 80 mM sodium borate buffer at pH 9.0 the addition of 1 μM **1-V2** results in ∼50% conversion of $[Ru(bpy)_3]^{3+}$ in 0.08 s, which is about 20 times faster than with 1 μM **1-P2** and more than 2 orders of magnitude faster than the self-decomposition rate of $[Ru(bpy)_3]^{3+}$ (Figure 2). For comparison, we also obtained the kinetics of $[Ru(bpy)_3]^{3+}$ reduction catalyzed by 5 μM $Co(NO_3)_2$ (1.25 equiv of cobalt relative to 1 μM **1-V2**), which exhibits a characteristic sigmoidal-shaped curve with an induction period (pink curve, Figure 2), indicating formation of catalytically active species from the initial $Co(NO_3)_2$.[52] The concentration of O_2 generated using 1 mM $[Ru(bpy)_3]^{3+}$ increases from about 0.15 to 0.18 mM with an increase of [**1-V2**] from 0.5 to 4.0 μM reaching the yield, $Y = 4[O_2]/[[Ru(bpy)_3]^{3+}]_0$ of 70 ± 5% (Figure S15). Based on the initial rate of $[Ru(bpy)_3]^{3+}$ consumption and the O_2 yields, the initial apparent turnover frequency, $TOF_{app} = \{0.7(d[Ru(bpy)_3{}^{3+}]/dt)\}/(4 \times [\mathbf{1\text{-}V2}])$, is in the range (1.6−2.2) × 10^3 s^{-1}, which is exceptionally fast. This value is considerably higher than that of the oxygen evolving center (OEC) in PSII (as high as 400 s^{-1}),[15] but direct comparison of the water oxidation rates of **1-V2** and the OEC is not highly meaningful because the overpotentials (driving forces) in these two systems are different. The kinetic and mechanistic analyses show that the initial reaction rate is close to first order with respect to $[\mathbf{1\text{-}V2}]_o$ and $[[Ru(bpy)_3]^{3+}]_o$ (at <1.0 mM) and approaching zero order with respect to $[[Ru(bpy)_3]^{3+}]_o$ (at >1.0 mM); see Figure S16.

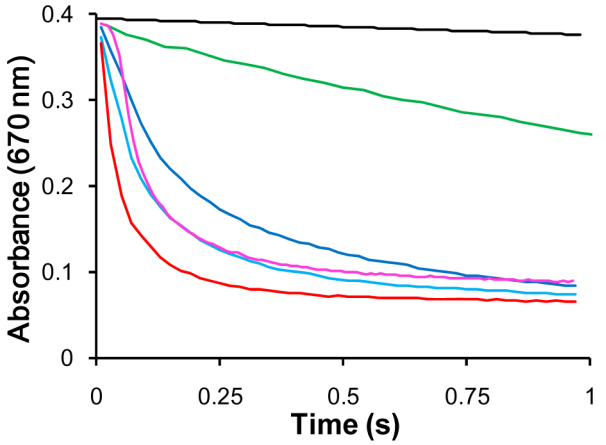

Figure 2. Kinetics of $[Ru(bpy)_3]^{3+}$ reduction to $[Ru(bpy)_3]^{2+}$ measured as the decrease in absorbance at 670 nm. No catalyst (black line), 1 μM **1-P2** (green curve), 0.5 μM **1-V2** (blue curve), 1 μM **1-V2** (light-blue curve), 2 μM **1-V2** (red curve) and 5 μM $Co(NO_3)_2$ (pink curve). Conditions: 1 mM $[Ru(bpy)_3]^{3+}$, 80 mM sodium borate buffer at pH 9.0, 298 K.

Given the importance of visible-light-driven catalytic water oxidation, the activity of **1-V2** was also assessed by the standard approach using $[Ru(bpy)_3]^{2+}$ as a photosensitizer and persulfate as a sacrificial electron acceptor (Figure 3).[32,53] The O_2 yield in the presence of **1-V2** is twice as high as that in the presence of **1-P2**[6,30] (Figure 3), indicating the higher selectivity for water oxidation versus bpy ligand oxidation for **1-**

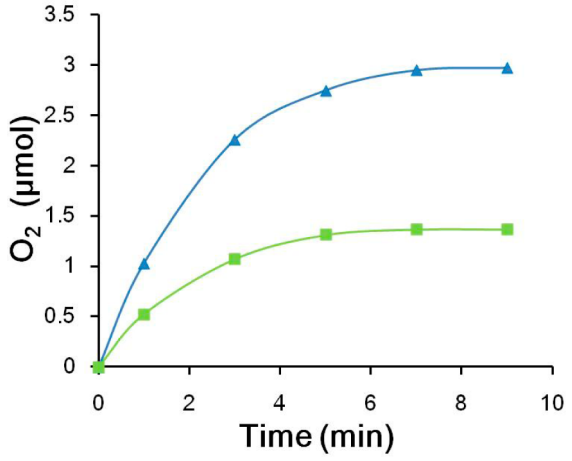

Figure 3. Time profile of light-driven O_2 evolution catalyzed by 2.0 μM **1-V2** (blue triangles) or 2.0 μM **1-P2** (green squares) with 1.0 mM $[Ru(bpy)_3]Cl_2$ and 5.0 mM $Na_2S_2O_8$. Conditions: 455 nm LED light (17 mW, beam diameter ∼0.4 cm), 80 mM sodium borate buffer initial pH 9.0, total solution volume 2.0 mL.

dx.doi.org/10.1021/ja5045488 | J. Am. Chem. Soc. 2014, 136, 9268−9271

V2. The quantum efficiency of O_2 formation at 6.0 μM **1-V2** reaches the very high value of ~68% (Table S5).

Note that the initial slopes (O_2 versus time) in the light-driven reactions are directly related to the quantum yield of these reactions; they are not the intrinsic catalytic turnover rates or TOF. Critically in light-driven reactions, the rate-limiting step in the great majority of cases (e.g., using the very popular $[Ru(bpy)_3]^{2+}$/light/persulfate system) is not the rate (TOF) of the catalyst. In contrast, the rate of oxidant, e.g. $[Ru(bpy)_3]^{3+}$, generation is rate limiting. As a consequence, catalyst efficiencies (TOF, etc.) usually cannot be assessed in light-driven reactions and in particular in light-driven multi-electron processes. The one rare exception for light-driven reactions in which the catalyst efficiency can be rate limiting or co-rate-limiting is where a very intense light source (not terrestrial sunlight) is used. To provide direct evidence for our case (**1-V2**/$[Ru(bpy)_3]^{2+}$/light/persulfate) that photogeneration of oxidant is rate limiting and catalyst turnover is not, we compare the accumulation of $[Ru(bpy)_3]^{3+}$ oxidant in both the presence and absence of **1-V2** by UV−vis spectroscopy. Figure S17 shows that the photogeneration of the $[Ru(bpy)_3]^{3+}$ oxidant in the absence of **1-V2** by UV−vis spectra after 30 s of irradiation. Importantly, in the presence of **1-V2**, all the photogenerated $[Ru(bpy)_3]^{3+}$ oxidant is efficiently and almost completely consumed by **1-V2** for catalytic water oxidation/O_2 generation. The inserted photos clearly show the formation of O_2 bubbles in the presence of **1-V2** but no O_2 bubbles in the absence of **1-V2**. A central consequence of rate-limiting oxidant generation in photodriven water oxidation processes is that the rate of O_2 generation does not reflect the TOF of the WOC.

The stability of **1-V2** was studied by multiple experiments. After 24 h no apparent changes in the UV−vis spectra are observed in water or in borate buffer (Figure S5). ^{51}V NMR spectra of **1-V2** in D_2O or in borate buffer at pH 9.0 exhibit only one peak at −506.8 ppm (Figure S6); no changes were noticed over a period of one month. In addition, heating the NMR sample to 80 °C followed by cooling to room temperature gives the same ^{51}V NMR spectrum (same chemical shift and line width; Figure S7), confirming the stability of **1-V2**. Moreover, FT-IR (Figure S8) and ^{51}V NMR (Figure 4) spectra show no changes in **1-V2** before and after light-driven catalysis.

Also, water oxidation catalyzed by **1-V2** and $Co(NO_3)_2$ in separate reactions exhibits different overall kinetic profiles and different initial rates (Figure S18). Table S4 gives many additional results from a range of stability experiments.[44,54,55] The catalytic water oxidation activity of 2 μM **1-V2** is higher than that of 8 μM Co^{2+}(aq) (same equivalents of Co species) under identical conditions (Figure S19). Furthermore, the dependence of catalytic water oxidation activity as a function of pH, buffer, and buffer concentration by **1-V2**, Co^{2+}(aq) and CoO_x are different (Table S4). In addition, a toluene solution of tetra-*n*-heptylammonium nitrate ($THpANO_3$) was used to quantitatively extract **1-V2** from the reaction (Figure S20). The extractive removal of **1-V2** from the solution after first catalytic run totally stops the reaction in the water layer (Figure S20). Similarly, control experiments show that the extraction of **1-V2** before catalytic reaction reduces the O_2 yield to almost zero. In contrast, neither CoO_x nor Co^{2+}(aq) is extracted into the toluene layer by $THpA^+$, and as a consequence, catalytic water oxidation is not affected significantly in these cases.[44] Finally, no particle formation is observed by dynamic light scattering for reactions catalyzed by **1-V2**; in contrast, particles with a size around 220 nm are formed in reactions catalyzed by Co^{2+}(aq) (Figure S21).

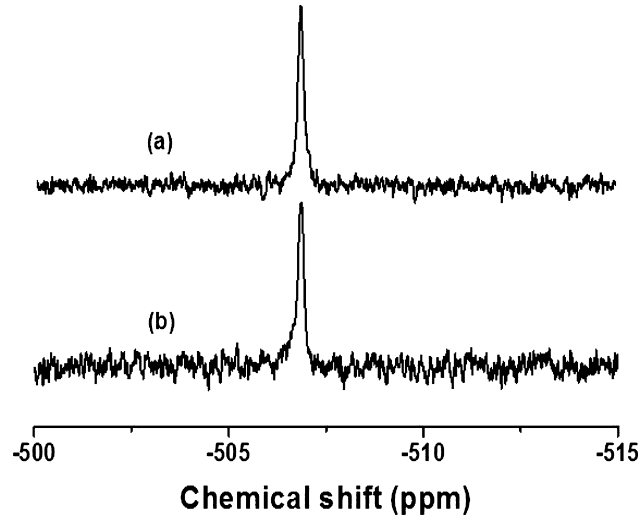

Figure 4. ^{51}V NMR for **1-V2** (a) before and (b) after the light-driven water oxidation reaction. Conditions: 455 nm LED light (17 mW, beam diameter ~0.4 cm), 3.3 mM $[Ru(bpy)_3]^{2+}$, 12.6 mM $Na_2S_2O_8$, 67 μM **1-V2**, 80 mM sodium borate buffer, initial pH 9.0, illumination time 50 min. TON ~ 35, chemical yield = 2 × (O_2)/($Na_2S_2O_8$) ≈ 37%. Chemical shifts are relative to neat $VOCl_3$ at 25 °C (0 ppm).

In conclusion, we report a new molecular carbon-free (oxidatively stable) water oxidation catalyst that exhibits high hydrolytic stability and is also exceptionally fast under mild conditions (TOF > 1 × 10^3 s^{-1}). Under light-driven conditions, **1-V2** exhibits higher selectivity for water oxidation versus bpy ligand oxidation, and the final O_2 yield using **1-V2** is twice as high as that using **1-P2**. In addition, the quantum efficiency of O_2 formation at 6.0 μM **1-V2** reaches the very high value of ~68%. Extensive studies confirm that the polyanion unit (**1-V2**) itself is the dominant active catalyst and not Co^{2+}(aq) or cobalt oxide.

■ ASSOCIATED CONTENT

Supporting Information

Experimental details and data. This material is available free of charge via the Internet at http://pubs.acs.org.

■ AUTHOR INFORMATION

Corresponding Author

chill@emory.edu

Author Contributions

⊥These authors contributed equally.

Notes

The authors declare no competing financial interest.

■ ACKNOWLEDGMENTS

The authors thank the U.S. Department of Energy, Office of Basic Energy Sciences, Solar Photochemistry program, grant no. DE-FG02-07ER15906 for support and also gratefully acknowledge NSF MRI-R2 grant (CHE-0958205) and the use of the resources of the Cherry Emerson Center for Scientific Computation. The authors thank Zhen Luo and Yong Ding for very preliminary activity evaluations.

REFERENCES

(1) Lewis, N. S.; Nocera, D. G. *Proc. Natl. Acad. Sci. U. S. A.* **2006**, *103*, 15729.
(2) Eisenberg, R.; Gray, H. B. *Inorg. Chem.* **2008**, *47*, 1697.
(3) Barber, J. *Chem. Soc. Rev.* **2009**, *38*, 185.
(4) Shevchenko, D.; Anderlund, M. F.; Thapper, A.; Styring, S. *Energy Environ. Sci.* **2011**, *4*, 1284.
(5) Hammarstrom, L.; Hammes-Schiffer, S. *Acc. Chem. Res.* **2009**, *42*, 1859.
(6) Yin, Q.; Tan, J. M.; Besson, C.; Geletii, Y. V.; Musaev, D. G.; Kuznetsov, A. E.; Luo, Z.; Hardcastle, K. I.; Hill, C. L. *Science* **2010**, *328*, 342.
(7) Huang, Z.; Luo, Z.; Geletii, Y. V.; Vickers, J.; Yin, Q.; Wu, D.; Hou, Y.; Ding, Y.; Song, J.; Musaev, D. G.; Hill, C. L.; Lian, T. *J. Am. Chem. Soc.* **2011**, *133*, 2068.
(8) Roeser, S.; Fàrrs, P.; Bozoglian, F.; Martínez-Belmonte, M.; Benet-Buchholz, J.; Llobet, A. *ChemSusChem* **2011**, *4*, 197.
(9) Hurst, J. K. *Coord. Chem. Rev.* **2005**, *249*, 313.
(10) Concepcion, J. J.; Jurss, J. W.; Brennaman, M. K.; Hoertz, P. G.; Patrocinio, A. O. T.; Iha, N. Y. M.; Templeton, J. L.; Meyer, T. J. *Acc. Chem. Res.* **2009**, *42*, 1954.
(11) Hull, J. F.; Balcells, D.; Blakemore, J. D.; Incarvito, C. D.; Eisenstein, O.; Brudvig, G. W.; Crabtree, R. H. *J. Am. Chem. Soc.* **2009**, *131*, 8730.
(12) Zong, R.; Thummel, R. *J. Am. Chem. Soc.* **2005**, *127*, 12802.
(13) McCool, N. S.; Robinson, D. M.; Sheats, J. E.; Dismukes, G. C. *J. Am. Chem. Soc.* **2011**, *133*, 11446.
(14) McDaniel, N. D.; Coughlin, F. J.; Tinker, L. L.; Bernhard, S. *J. Am. Chem. Soc.* **2008**, *130*, 210.
(15) Duan, L.; Bozoglian, F.; Mandal, S.; Stewart, B.; Privalov, T.; Llobet, A.; Sun, L. *Nat. Chem.* **2012**, *4*, 418.
(16) Muckerman, J. T.; Polyansky, D. E.; Wada, T.; Tanaka, K.; Fujita, E. *Inorg. Chem.* **2008**, *47*, 1787.
(17) Masaoka, S.; Sakai, K. *Chem. Lett.* **2009**, *38*, 182.
(18) Kanan, M. W.; Nocera, D. G. *Science* **2008**, *321*, 1072.
(19) Robinson, D. M.; Go, Y. B.; Greenblatt, M.; Dismukes, G. C. *J. Am. Chem. Soc.* **2010**, *132*, 11467.
(20) Youngblood, W. J.; Lee, S.-H. A.; Kobayashi, Y.; Hernandez-Pagan, E. A.; Hoertz, P. G.; Moore, T. A.; Moore, A. L.; Gust, D.; Mallouk, T. E. *J. Am. Chem. Soc.* **2009**, *131*, 926.
(21) Jiao, F.; Frei, H. *Angew. Chem., Int. Ed.* **2009**, *48*, 1841.
(22) Barnett, S. M.; Goldberg, K. I.; Mayer, J. M. *Nat. Chem.* **2012**, *4*, 498.
(23) Zidki, T.; Zhang, L.; Shafirovich, V.; Lymar, S. V. *J. Am. Chem. Soc.* **2012**, *134*, 14275.
(24) Indra, A.; Menezes, P. W.; Zaharieva, I.; Baktash, E.; Pfrommer, J.; Schwarze, M.; Dau, H.; Driess, M. *Angew. Chem., Int. Ed.* **2013**, *52*, 13206.
(25) Smith, R. D. L.; Prévot, M. S.; Fagan, R. D.; Zhang, Z.; Sedach, P. A.; Siu, M. K. J.; Trudel, S.; Berlinguette, C. P. *Science* **2013**, *340*, 60.
(26) Liu, H.; Patzke, G. R. *Chem. – Asian J.* **2014**, DOI: 10.1002/asia.201400140.
(27) Kim, T. W.; Choi, K.-S. *Science* **2014**, *343*, 990.
(28) Vannucci, A. K.; Alibabaei, L.; Losego, M. D.; Concepcion, J. J.; Kalanyan, B.; Parsons, G. N.; Meyer, T. J. *Proc. Natl. Acad. Sci. U. S. A.* **2013**, *110*, 20918.
(29) Wang, D.; Groves, J. T. *Proc. Natl. Acad. Sci. U. S. A.* **2013**, *110*, 15579.
(30) Geletii, Y. V.; Botar, B.; Kögerler, P.; Hillesheim, D. A.; Musaev, D. G.; Hill, C. L. *Angew. Chem., Int. Ed.* **2008**, *47*, 3896.
(31) Sartorel, A.; Carraro, M.; Scorrano, G.; Zorzi, R. D.; Geremia, S.; McDaniel, N. D.; Bernhard, S.; Bonchio, M. *J. Am. Chem. Soc.* **2008**, *130*, 5006.
(32) Geletii, Y. V.; Huang, Z.; Hou, Y.; Musaev, D. G.; Lian, T.; Hill, C. L. *J. Am. Chem. Soc.* **2009**, *131*, 7522.
(33) Toma, F. M.; Sartorel, A.; Iurlo, M.; Carraro, M.; Parisse, P.; Maccato, C.; Rapino, S.; Gonzalez, B. R.; Amenitsch, H.; Ros, T. D.; Casalis, L.; Goldoni, A.; Marcaccio, M.; Scorrano, G.; Scoles, G.; Paolucci, F.; Prato, M.; Bonchio, M. *Nat. Chem.* **2010**, *2*, 826.
(34) Besson, C.; Huang, Z.; Geletii, Y. V.; Lense, S.; Hardcastle, K. I.; Musaev, D. G.; Lian, T.; Proust, A.; Hill, C. L. *Chem. Commun.* **2010**, 2784.
(35) Murakami, M.; Hong, D.; Suenobu, T.; Yamaguchi, S.; Ogura, T.; Fukuzumi, S. *J. Am. Chem. Soc.* **2011**, *133*, 11605.
(36) Zhu, G.; Geletii, Y. V.; Kögerler, P.; Schilder, H.; Song, J.; Lense, S.; Zhao, C.; Hardcastle, K. I.; Musaev, D. G.; Hill, C. L. *Dalton Trans.* **2012**, *41*, 2084.
(37) Zhu, G.; Glass, E. N.; Zhao, C.; Lv, H.; Vickers, J. W.; Geletii, Y. V.; Musaev, D. G.; Song, J.; Hill, C. L. *Dalton Trans.* **2012**, *41*, 13043.
(38) Tanaka, S.; Annaka, M.; Sakai, K. *Chem. Commun.* **2012**, *48*, 1653.
(39) Car, P.-E.; Guttentag, M.; Baldridge, K. K.; Albertoa, R.; Patzke, G. R. *Green Chem.* **2012**, *14*, 1680.
(40) Lv, H.; Geletii, Y. V.; Zhao, C.; Vickers, J. W.; Zhu, G.; Luo, Z.; Song, J.; Lian, T.; Musaev, D. G.; Hill, C. L. *Chem. Soc. Rev.* **2012**, *41*, 7572.
(41) Goberna-Ferrón, S.; Vigara, L.; Soriano-López, J.; Galán-Mascarós, J. R. *Inorg. Chem.* **2012**, *51*, 11707.
(42) Soriano-López, J.; Goberna-Ferrón, S.; Vigara, L.; Carbó, J. J.; Poblet, J. M.; Galán-Mascarós, J. R. *Inorg. Chem.* **2013**, *52*, 4753.
(43) Song, F.; Ding, Y.; Ma, B.; Wang, C.; Wang, Q.; Du, X.; Fu, S.; Song, J. *Energy Environ. Sci.* **2013**, *6*, 1170.
(44) Vickers, J. W.; Lv, H.; Sumliner, J. M.; Zhu, G.; Luo, Z.; Musaev, D. G.; Geletii, Y. V.; Hill, C. L. *J. Am. Chem. Soc.* **2013**, *135*, 14110.
(45) Sumliner, J. M.; Lv, H.; Fielden, J.; Geletii, Y. V.; Hill, C. L. *Eur. J. Inorg. Chem.* **2014**, 635.
(46) Vickers, J. W.; Sumliner, J. M.; Lv, H.; Morris, M.; Geletii, Y. V.; Hill, C. L. *Phys. Chem. Chem. Phys.* **2014**, *16*, 11942.
(47) Han, X.-B.; Zhang, Z.-M.; Zhang, T.; Li, Y.-G.; Lin, W.; You, W.; Su, Z.-M.; Wang, E.-B. *J. Am. Chem. Soc.* **2014**, *136*, 5359.
(48) Guo, S.-X.; Liu, Y.; Lee, C.-Y.; Bond, A. M.; Zhang, J.; Geletii, Y. V.; Hill, C. L. *Energy Environ. Sci.* **2013**, *6*, 2654.
(49) Quintana, M.; López, A. M.; Rapino, S.; Toma, F. M.; Iurlo, M.; Carraro, M.; Sartorel, A.; Maccato, C.; Ke, X.; Bittencourt, C.; Da Ros, T.; Van Tendeloo, G.; Marcaccio, M.; Paolucci, F.; Prato, M.; Bonchio, M. *ACS Nano* **2013**, *7*, 811.
(50) Li, B.; Yan, Y.; Li, F.; Xu, L.; Bi, L.; Wu, L. *Inorg. Chim. Acta* **2009**, 2796.
(51) Ghosh, P. K.; Brunschwig, B. S.; Chou, M.; Creutz, C.; Sutin, N. *J. Am. Chem. Soc.* **1984**, *106*, 4772.
(52) Vickers, J.; Lv, H.; Zhuk, P. F.; Geletii, Y. V.; Hill, C. L. *MRS Proceedings* **2012**, *1387*, mrsf11−1387−e02−01.
(53) White, H. S.; Becker, W. G.; Bard, A. J. *J. Phys. Chem.* **1984**, *88*, 1840.
(54) Schiwon, R.; Klingan, K.; Dau, H.; Limberg, C. *Chem. Commun.* **2014**, *50*, 100.
(55) Stracke, J. J.; Finke, R. G. *ACS Catal.* **2014**, *4*, 79.